DOI: 10.13009/EUCASS2023-345
Aerospace Europe Conference 2023 – 10TH EUCASS – 9TH CEAS

Comparison of Tiltrotor Whirl Flutter Analyses with Gimballed and Hingeless Hub Models

Ui-Jin Hwang, Jae-Sang Park*† and Myeong-Kyu Lee***
** Chungnam National University*
99 Daehak-ro Yuseong-gu Daejeon, Republic of Korea
99uj0630@o.cnu.ac.kr
† aerotor@cnu.ac.kr
*** Korea Aerospace Research Institute*
169-84 Gwahak-ro Yuseong-gu Daejeon, Republic of Korea
mklee@kari.re.kr

Abstract
This study investigates and compares the whirl flutter characteristics of two different hub models, gimballed and hingeless hubs, for a tiltrotor aircraft in cruise flight. This study uses the rotorcraft comprehensive analysis code CAMRAD II to model the proprotor, semi-span wing, and pylon, and analyzes the aeroelastic instability of a tiltrotor system. The proprotor frequency characteristics depend on the hub type and have influence on the wing-rotor interaction to cause whirl flutter. It is shown that the rotor regressive lag mode frequency is an important system design parameter for a hingeless tiltrotor, whereas the rotor regressive gimbal mode is important for a gimballed tiltrotor.

1. Introduction

A tiltrotor aircraft can convert between helicopter (Figure 1(a)) and airplane (Figure 1(b)) flight modes by rotating the proprotors located at the wing tips by 90°. These tiltrotors are capable of vertical take-off and landing, and hovering, as well as faster flight speeds and longer ranges than conventional helicopters. This capability makes tiltrotors attractive aircraft for the military as utility and attack helicopters, and civil applications, such as electric vertical take-off and landing (e-VTOL). In February 2022, the U.S. Army selected Bell's V-280 Valor tiltrotor (Figure 1) as the Future Long-Range Assault Aircraft (FLRAA), which will eventually replace the UH-60 Black Hawks [1]. The decision of the U.S. is expected to have a significant impact on future global vertical lift aircraft development trends. However, in the tiltrotor airplane mode, the maximum flight speed, which is a major concern for tiltrotor aircraft designs, is limited by whirl flutter stability. Whirl flutter is an aeroelastic instability phenomenon of tiltrotors in airplane mode, which is caused by the coupled motions of the proprotor and the flexible wing/pylon structure at high-speed conditions [2]. Classical whirl flutter, the fundamental concept of whirl flutter in tiltrotors, was first analytically discovered by Taylor and Browne [3]. This theoretical problem became a reality when the Lockheed L-188 Electra, a turboprop airliner, experienced two fatal crashes in September 1959 and March 1960. After these accidents, whirl flutter studies of turboprop airliner wing mounted propellers were conducted extensively. However, in the case of tiltrotors, the proprotor for hovering flight performance is more flexible and larger than the propeller for turboprop aircraft. Furthermore, there is a need to rotate the pylon for conversion between helicopter and airplane modes, creating natural flexibility in the pitch [4]. Thus, this differs from the relatively simple classical whirl flutter interpretation with two degrees of freedom: rigid blades, hub, and flexible engine mounting; tiltrotor whirl flutter analyses use more degrees of freedom and are more complex [5]. Therefore, whirl flutter studies of tiltrotors are important and should be conducted in detail.
Currently, the primary objective of tiltrotor design is to increase the maximum flight speed and reduce the weight of tiltrotors by modifying the blades, wings, or hubs. Tiltrotor aircraft generally use a stiff in-plane gimballed rotor; however, recently, attempts have been made to change to a hingeless rotor. Gimballed hubs have been used because they have less vibration than articulated hubs, and most stiff in-plane rotors can avoid ground resonance. However, there is a disadvantage of significant in-plane dynamic blade loads during maneuvers [6]. A hingeless hub is simpler and lighter than a gimballed hub, resulting in reduced structural weight and improved aircraft agility [7]. Another advantage is the enhanced control response and ease of maintenance [8]. In addition, hingeless soft in-plane rotors can significantly reduce the in-plane blade loads in the tiltrotor, thereby reducing hub strength requirements. There have been many previous whirl flutter analyses of gimballed proprotors, but few have focused on hingeless proprotors. In 1956, the whirl flutter of the tiltrotor first occurred during XV-3 flight tests using an articulated rotor [9]. Subsequently,

DOI: 10.13009/EUCASS2023-345

the XV-3 rotor was replaced with a stiff in-plane teetering rotor and the mechanism of whirl flutter for tiltrotor aircraft was understood via wind tunnel and flight tests [10]. A comprehensive aeroelastic instability analysis technique for a tiltrotor was developed for Bell's stiff in-plane gimballed rotor and Boeing's soft in-plane hingeless rotor [5]. Considerable experimental and analytical studies have been conducted on the whirl flutter of gimballed rotors, such as XV-15 [11], WRATS [12], and V-22 [13]. The U.S. Army and NASA developed the TiltRotor Aeroelastic Stability Testbed (TRAST), which can accommodate both gimballed and hingeless hubs [4, 7, 14-15]. In these previous studies, numerical whirl flutter analyses were performed extensively for both gimballed and hingeless tiltrotors. However, a whirl flutter comparison study between the two hub models was not conducted because the two tiltrotors had different blade models. The University of Maryland most recently tested tiltrotors in wind tunnels, and aeroelastic stability test data were collected for gimballed and hingeless tiltrotors [16]. However, even in this previous study [16], a comparison of whirl flutter characteristics for different hub types was not conducted. Therefore, to use hingeless rotors instead of gimballed rotors in future tiltrotors, a study is required to understand the whirl flutter characteristics of hingeless proprotors compared with those of gimballed proprotors.
Therefore, this study compares whirl flutter analyses with two different hub types, namely, gimballed and hingeless hubs; however, identical proprotor blade and wing/pylon models are used between the two hub models. In addition, for whirl flutter analyses, this study uses two baseline tiltrotors, namely, the proprotor and wing/pylon model of the TRAST hingeless rotor in a previous study by the U.S. Army/NASA [7] and the unmanned tiltrotor aircraft developed by KARI (Korea Aerospace Research Institute) [17-18]. The rotorcraft comprehensive analysis code, CAMRAD II, is used for whirl flutter analyses. This study numerically investigates and compares the whirl flutter characteristics of the gimballed and hingeless proprotors of a tiltrotor aircraft.

(a) Helicopter mode

(b) Airplane mode

Figure 1: V-280 Valor tiltrotor

2. Analytical Modeling

2.1 Tiltrotor models

This study uses two baseline tiltrotor models including the proprotor and semi-span wing/pylon systems. The first baseline model is a U.S. Army/NASA TRAST with a hingeless hub [7] and the second baseline model is a KARI TRS tiltrotor, which uses a gimballed hub [17-18]. In this study, the gimballed and hingeless hub models are newly considered to TRAST and TRS tiltrotors, respectively. Table 1 lists the general properties of the tiltrotors used in this study.

Table 1: Description of the tiltrotor models

	TRAST	KARI TRS
Baseline hub type	Hingeless	Gimbal
Number of blades	3	3
Hover RPM	888	1605
Cruise RPM	742	1284

DOI: 10.13009/EUCASS2023-345

Blade radius, ft	4	4.7
Blade mean chord, ft	0.5	0.63
Blade pre twist, deg	−40, linear	-38.3, nonlinear
Airfoil	64-x08, 64-x12, 64-x18, 64-x25	SF08, SF12, SF18, SF25, SF30
Precone, deg	2.5	2
Undersling, %R	0	-0.021 (Gimbal) 0 (Hingeless)
Wing semi-span length, ft	4.4	6.56

2.2 Aeroelastic modeling and analytical techniques

The present study uses the rotorcraft comprehensive analysis code CAMRAD II to model the proprotor, semi-span wing, and pylon, and to analyze the whirl flutter stability of tiltrotors. The proprotor blade structural dynamics is modeled using nonlinear finite beam elements. Each blade has 15 and eight finite beam elements for the TRAST and TRS proprotors, respectively. Rotor control systems, including swashplates, pitch links, and pitch horns, are also modeled in both rotor models. Airfoil tables, including airfoil aerodynamic coefficients, are used for blade aerodynamics modeling in CAMRAD II. The blade unsteady aerodynamic loads are calculated using lifting-line theory. In this study, 21 and 20 aerodynamic panels are used for the TRAST and TRS rotor blades, respectively. For modeling of the semi-span wing with a pylon, natural frequencies and mode shape vectors are applied to the TRAST model [7]; however, 20 nonlinear finite beam elements are used for the TRS model. Figure 2 illustrates the CAMRAD II model of the TRAST and TRS tiltrotors. The wing of the TRAST model is not shown Figure 2(a) because the airframe dynamics are represented by an orthogonal modal model, which includes the natural frequencies and mode shapes obtained from the previous study [7]. For both proprotor models in airplane mode, the uniform inflow model is applied. The proprotor is first trimmed to zero torque at a given flight speed to represent the windmill state, which is the most severe flight condition for whirl flutter. Subsequently, using eigenvalue analysis, the frequency and damping of the aeroelastic system of the coupled proprotor and wing/pylon are calculated.

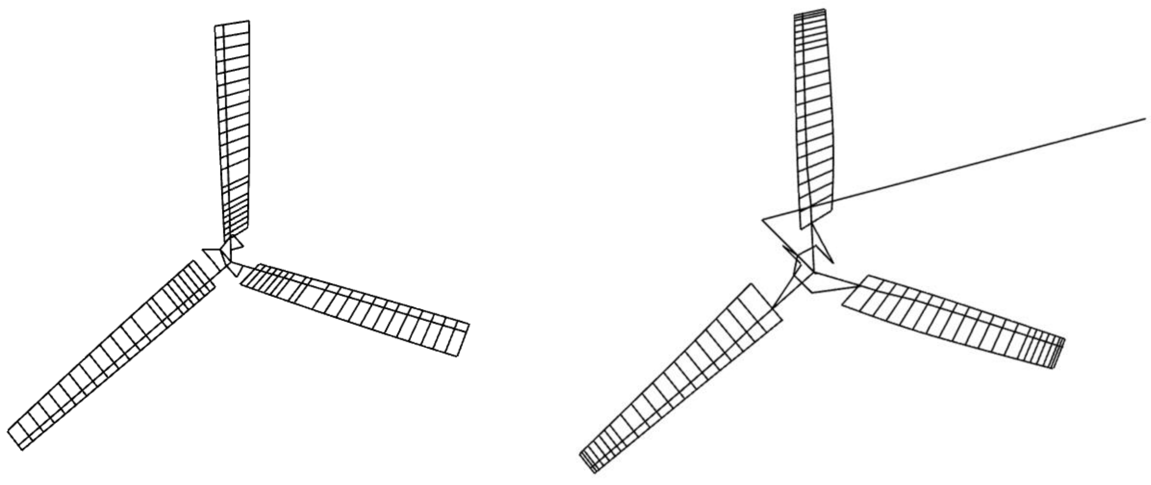

(a) TRAST proprotor (b) TRS proprotor/wing/pylon

Figure 2: CAMRAD II models of TRAST and TRS tiltrotors in airplane mode

DOI: 10.13009/EUCASS2023-345

3. Numerical Results and Discussions

3.1 Natural frequency analyses

The rotating blade and wing/pylon natural frequency results are predicted and shown in Figure 3 and Table 2, respectively. The rotating blade natural frequencies in terms of the rotor rotational speed are calculated for the gimballed and hingeless hub models (Figure 3). In the figure, one-per-rev (1/rev or 1P) indicates the non-dimensional rotor rotational speed. Collective pitch control angles (θ_0) of 0° and 10° are used for TRAST and TRS, respectively. In this study, the first flap and lag modes are defined in the collective mode at the rotor speed in airplane mode; however, the gimbal mode is calculated in the cyclic mode at the rotor speed in airplane mode. The natural frequencies of a rotating blade of the proprotor are compared to the previous predictions [7, 18] to validate the rotor structural dynamics, as shown in Figure 3. For both rotor models, the predicted rotating natural frequencies in the collective mode (Figure 3(a), (c), and (e)) are matched well with the analysis results in previous studies [7, 18]. The natural frequencies in the cyclic mode (Figure 2(f)) are similar to those in previous studies [18]. However, for the results of the TRAST, the rotor frequency in the cyclic mode is not given in the reference [7]; hence, only a comparison with results in the collective mode is provided in this paper. Therefore, it is believed that the present structural dynamics modeling for TRAST and TRS proprotors is reasonable and acceptable. In addition, it is found that the rotating frequencies with hingeless and gimbal hubs in collective mode are very similar to each other for both the TRAST and TRS proprotor models. Table 2 lists the modal frequency characteristics of the wing/pylon models. The frequencies of the TRAST model are provided in a previous study [7], and those of the TRS model are calculated in the present study.

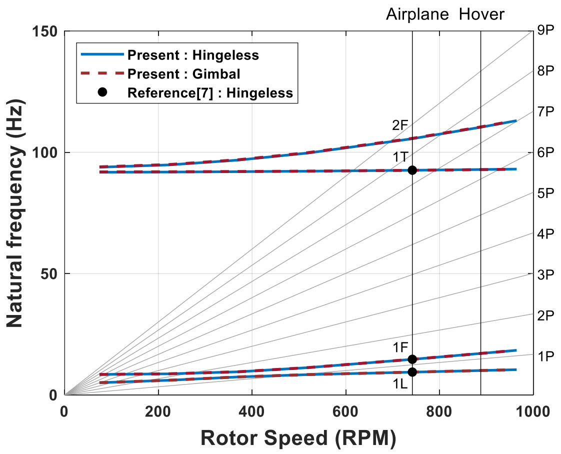

(a) TRAST soft in-plane rotor fan plot : collective mode

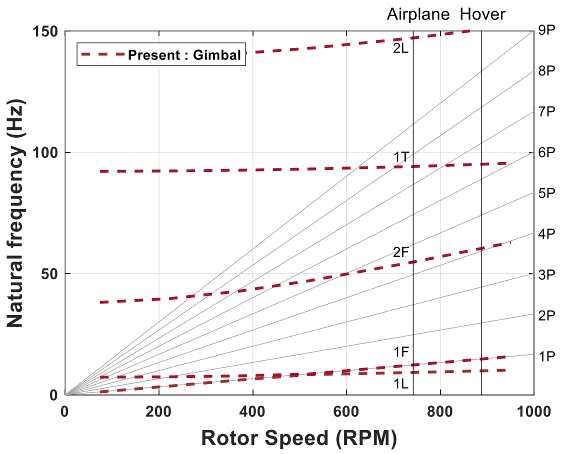

(b) TRAST soft in-plane gimballed rotor fan plot : cyclic mode

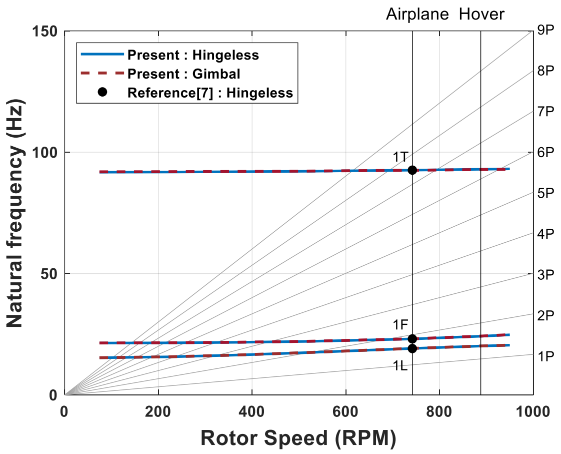

(c) TRAST stiff in-plane rotor fan plot : collective mode

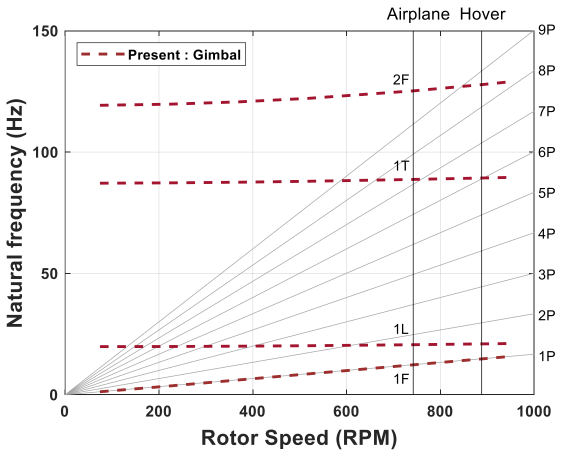

(d) TRAST stiff in-plane gimballed rotor fan plot : cyclic mode

DOI: 10.13009/EUCASS2023-345

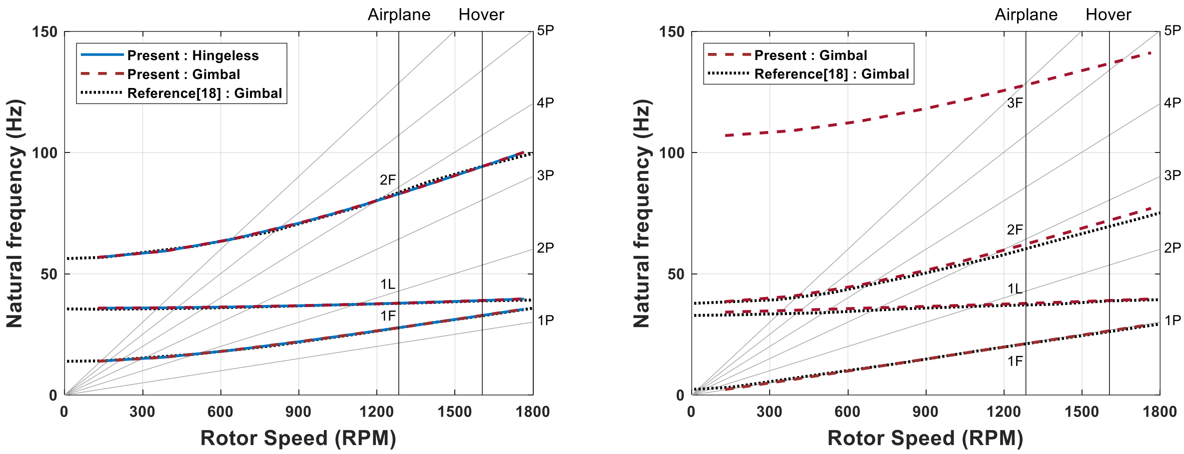

(e) TRS fan plot : collective mode (f) TRS gimballed rotor fan plot : cyclic mode

Figure 3: Fan plot analyses

Table 2: The fundamental mode natural frequencies of wing/pylon

	Wing beam , Hz	**Wing chord , Hz**	**Wing torsion , Hz**	**Pylon yaw , Hz**
TRAST generic wing/pylon	3.43	6.83	8.63	14.67
KARI TRS	6.30	5.55	20.08	34.88

3.2 Validation of whirl flutter analysis

This section validates the present whirl flutter analysis techniques with the previous works [7,16]. Figure 4 shows the predicted frequency and damping variations of the TRAST soft in-plane hingeless rotor with a generic wing/pylon model in terms of wind speed. The dashed lines are from the previous analysis results [7] using RCAS (Rotorcraft Comprehensive Analysis System), rotorcraft comprehensive analysis code, and the dash-dotted lines show the UMARC II (University of Maryland Advanced Rotorcraft Code) analyses [16]. The solid lines show the results of the present study using CAMRAD II. Figure 4(a) shows the frequencies of the wing and rotor in the two and three lower modes, respectively. The rotor modes are defined [5] based on the first mode frequency (ν/rev). There are a rotor regressive mode with a low frequency (ν-1) and a rotor progressive mode with a high frequency (ν+1). The rotor collective rotor modes are described using the collective flap (ν_β) and lag (ν_ζ) modes. For the gimballed hub, the coning (ν_β) mode is used. In this section, the rotor regressive lag mode is defined using (1- ν_ζ) because of a soft in-plane rotor (ν_ζ less than 1/rev). As shown in the figure, the frequency variation is in good agreement with all previous predictions for the wing beam and chord modes. A similar trend in the rotor regressive flap mode is observed. There are moderate differences in the rotor regressive lag modes; however, the overall variation in this study is similar to that in other analysis results. For the results using RCAS, the rotor frequency in the collective lag mode is not given in the reference [7]; therefore, only a comparison with the UMARC II results [16] is provided. Although there are discrepancies after 120 knots, the rotor collective lag mode and wing chord mode cross over at 90 and 100 knots, respectively, in the UMARC II and CAMRAD II results. The sign change of damping with wind speed is typically used to determine the whirl flutter occurrence of a tiltrotor. Figure 4(b) shows the damping variation in the two lowest wing modes (wing beam and chord modes). The damping values in the other modes, including the rotor modes, are significantly higher; therefore, they are not included in the figure. Although there are differences in the predicted damping values, the trends are similar. The wing beam mode is already unstable at 30 knots in all analyses but becomes stable at 50, 45, and 75 knots in the RCAS, UMARC II, and present CAMRAD II analyses, respectively. In contrast, in the wing chord mode, at 80, 70, and 85 knots, the sign of the damping changes (from positive to negative) and becomes unstable. Thus, the whirl flutter speeds of the TRAST soft in-plane hingeless model is calculated to be 80, 70, and 85 knots for the RCAS, UMARC II, and present CAMRAD II predictions, respectively. The results of the present study differ slightly from those of the RCAS and UMARC II by 5 and 15 knots, respectively; therefore, the present modeling and analysis techniques are appropriate for predicting the whirl flutter of a tiltrotor. Furthermore, similar to the prediction of

DOI: 10.13009/EUCASS2023-345

UMARC II, this study shows that the wing chord mode becomes unstable before the wing chord and rotor collective lag modes cross each other.

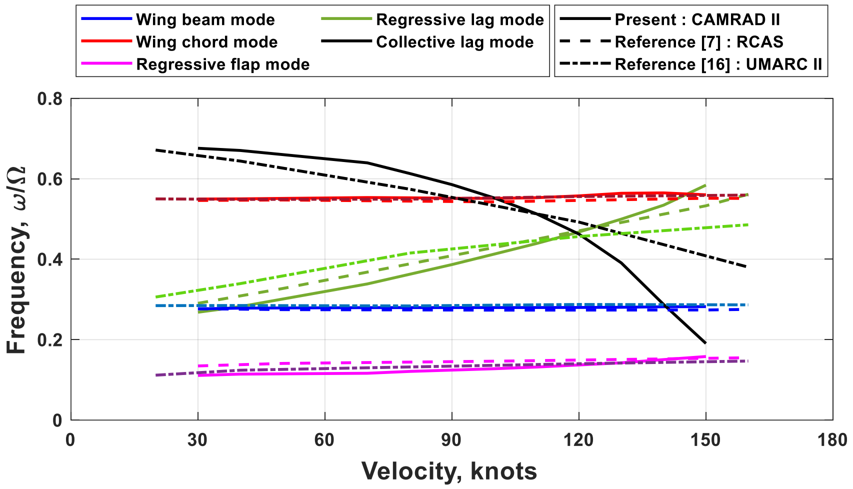

(a) Frequency

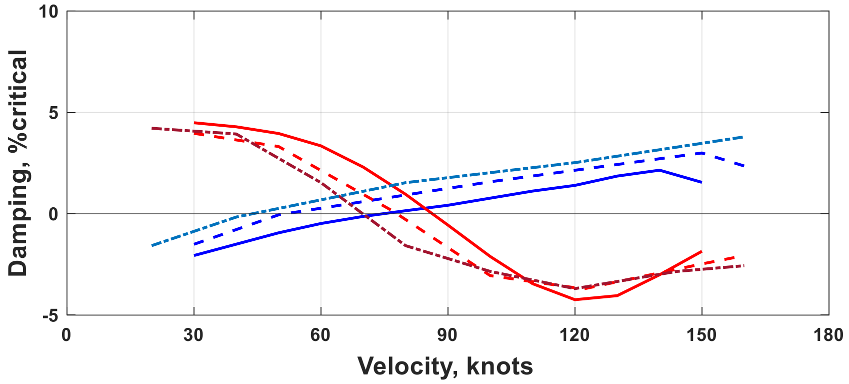

(b) Damping

Figure 4: Validation of whirl flutter analysis for TRAST soft in-plane hingeless tiltrotor

3.3 Whirl flutter analyses using soft in-plane tiltrotor

In this section, the proprotor and semi-span wing/pylon models described in the previous section with TRAST are modified using a gimballed hub. As previously explained, the models of the blade and wing/pylon are identical to those described in the previous section using a hingeless hub. Figure 5 shows a comparison of the whirl flutter characteristics of the hingeless (solid lines) and gimballed (dashed lines) models. In Figure 5(a), a rotor regressive gimbal mode is newly observed, unlike the results in the previous section. As shown in the figure, for the hingeless rotor model, the frequency in the wing beam mode is close to that in the rotor regressive lag mode at 30 knots, which leads to whirl flutter instability in the lower wind speed region. As described in the previous section, the whirl flutter occurs at 85 knots owing to the negative damping value in the wing chord mode. However, the rotor regressive flap, regressive lag, and collective lag modes using the hingeless hub are highly damped in the wind speed range examined (Figure 5(b)). Similar to the results for the hingeless hub, for the gimballed hub model, the wing beam mode is already unstable in the lower wind speed region. This is because the frequency in the wing beam mode is close to that in the rotor regressive lag mode, as shown in Figure 5(a). The wing beam mode with the gimballed hub is stabilized after 90 knots; however,

DOI: 10.13009/EUCASS2023-345

this result is slower than that obtained using the hingeless hub. The wing chord mode with the soft in-plane gimballed rotor becomes unstable at 95 knots, which is approximately 10 knots later than the result obtained using the hingeless hub model (Figure 5(b)). This is because the interaction between the wing chord and rotor collective lag modes occurs approximately 10 knots later than that of the hingeless hub. However, unlike a hingeless rotor, where all rotor modes are stable, for the gimballed hub model, the damping in the rotor regressive lag mode decreases sharply after 50 knots, resulting in negative values at 55 knots. This seems to be caused by the intersection of the rotor regressive gimbal mode and rotor regressive lag mode at 45 knots (Figure 5(a)). As the rotor regressive gimbal mode has a higher damping value, it is not plotted in Figure 5(b). Thus, the whirl flutter speed of the TRAST soft in-plane hingeless model is calculated to be 85 knots in the wing chord mode; however, the rotor instability speed for the TRAST soft in-plane gimballed model is calculated to be 55 knots in the rotor regressive lag mode.

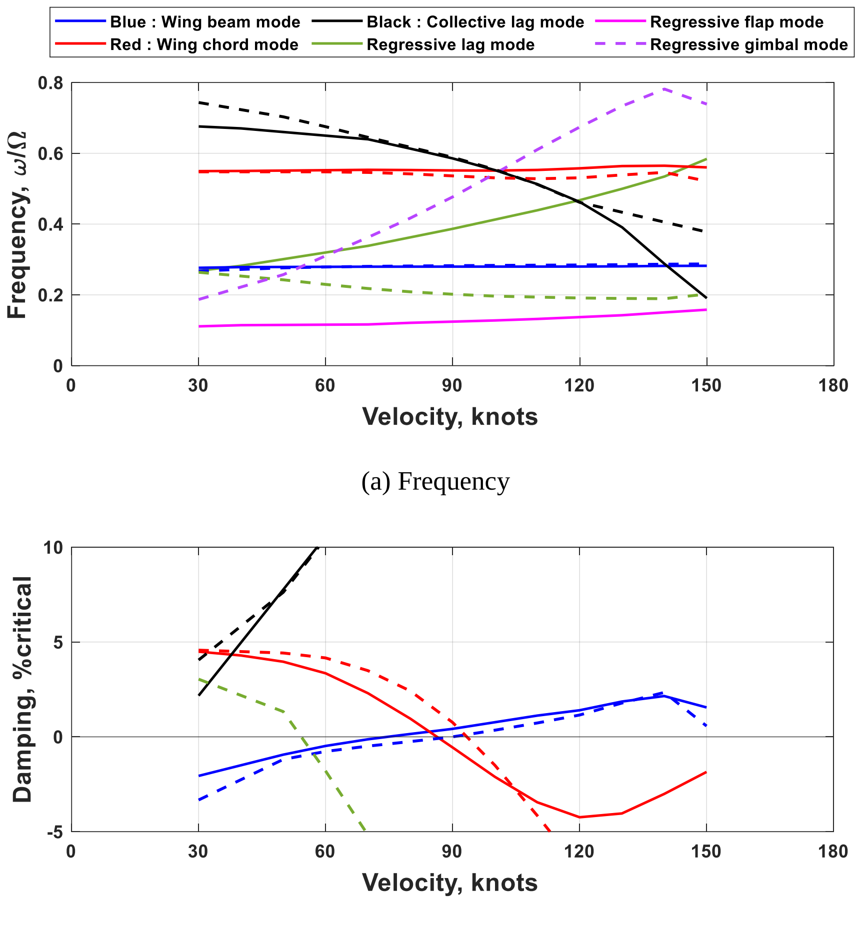

(b) Damping

Figure 5: Whirl flutter analysis results for TRAST soft in-plane hingeless and gimballed tiltrotors (solid line : hingeless rotor, dashed line : gimballed rotor)

3.4 Whirl flutter analyses using stiff in-plane tiltrotor

This section discusses the whirl flutter analyses of stiff in-plane rotors for the two hub types. In the first case, the TRAST stiff in-plane hingeless rotor and generic wing/pylon model [7] is used as a baseline model. Figure 6 shows a comparison of the whirl flutter predictions for the hingeless (solid lines) and gimballed hub models (dashed lines). Figure 6 shows the frequency and damping variations of the wing and rotor modes plotted against the wind speed. The results include the wing beam, chord, and torsion modes, and one rotor mode (regressive lag mode) for the hingeless rotor. However, the rotor regressive gimbal mode, instead of the wing torsion mode, is plotted for the results obtained using the gimballed hub because of its much lower frequency. For the hingeless stiff in-plane rotor model, the rotor

DOI: 10.13009/EUCASS2023-345

regressive lag mode is highly damped, and those damping values are outside the range indicated in the figure. However, whirl flutter in the wing beam mode occurs at 170 knots as the rotor regressive lag mode approaches the frequency in the wing beam mode after 150 knots. The whirl flutter speed is 170 knots, near 179 knots, where the frequencies in the wing beam and rotor regressive lag modes cross over. Furthermore, the study shows that damping in the wing chord mode increases and that in the wing torsion mode decreases (Figure 6(b)), while the frequencies in the wing chord and torsion modes cross at 160 knots (Figure 6(a)), which indicates a complex aeroelastic phenomenon. For the gimballed stiff in-plane rotor model, the frequency tendency of the rotor regressive lag modes differs from that of the hingeless rotor, and the rotor regressive gimbal mode is newly observed. The wing mode frequencies are similarly calculated for both hub models. For the gimballed rotor, the wing beam mode becomes unstable at about 85 knots, which is approximately 85 knots faster than the result for the hingeless hub model. The wing beam and rotor regressive gimbal modes intersect at 60 knots, as shown in Figure 6(a), causing a whirl flutter at 85 knots. In addition, the rotor regressive gimbal mode affects the wing chord mode because the frequency in the rotor regressive gimbal mode crosses that of the wing chord mode at 95 knots, leading to a rapid decrease in damping in the wing chord mode. However, the rotor regressive gimbal and lag modes are sufficiently damped in the wind speed range.

Next, the whirl flutter characteristics of another stiff in-plane tiltrotor model, the TRS stiff in-plane gimballed rotor, coupled with its wing/pylon model, are investigated. Figure 7 shows the frequency and damping values for the TRS stiff in-plane rotor and wing modes. The results include the wing beam and chord modes and two rotor modes (or the gimbal mode) for the hingeless and gimballed hub models. For the gimballed stiff in-plane rotor, the damping value in the wing chord mode decreases after the rotor regressive gimbal and wing chord modes cross over at 300 knots. Subsequently, the wing chord mode becomes unstable at 360 knots. Thus, the whirl flutter speed of the TRS stiff in-plane gimballed model is calculated to be 360 knots in the wing chord mode. The rotor regressive flap mode is more damped, as shown in Figure 7(b). However, for the hingeless tiltrotor model, whirl flutter occurs at 310 knots in the wing chord mode. The whirl flutter speed of the hingeless rotor is 50 knots lower than that of the gimballed rotor. Instability of the wing chord mode occurs because the frequency in the rotor regressive lag mode decreases as the flight speed increases and affects the wing chord mode. It can be represented that the rotor regressive lag mode contributes significantly to the instability of the wing chord mode. However, the rotor regressive lag mode is sufficiently damped as the flight speed increases.

Comparing the results of the whirl flutter analyses for the two stiff in-plane rotor models, the whirl flutter speeds are high for the TRAST hingeless and gimballed TRS models. In other words, the whirl flutter speed is higher for each baseline hub model than for the modified model. This is because the frequency gaps between the rotor and wing modes of the TRAST and TRS baseline models differ slightly. In addition, the frequency variation in the rotor regressive gimbal mode is different. In the TRS gimballed hub model, the frequency in the rotor regressive gimbal mode gradually increases, causing a delay in the cross-over speed between the wing chord and rotor regressive gimbal modes. The frequency in the rotor regressive gimbal mode for the TRAST gimballed hub increases relatively steeply in the lower wind speed region. However, it is evident that the frequency variation in the rotor modes differs depending on the hub type. Hence, in the wing-rotor interaction that causes whirl flutter, the hub type influences the occurrence of whirl flutter by changing the frequency variation in the rotor modes. For the hingeless hub models, a significant impact of the rotor regressive lag mode on the wing modes is evident in both the TRAST and TRS tiltrotors. By contrast, for the gimballed rotor, the wing mode instability is caused by the frequency cross-over between the rotor regressive gimbal mode and the wing modes. Therefore, the wing-rotor interaction behavior that leads to whirl flutter differs depending on the type of rotor hub. Finally, the damping in the rotor mode is stable within the air-speed range.

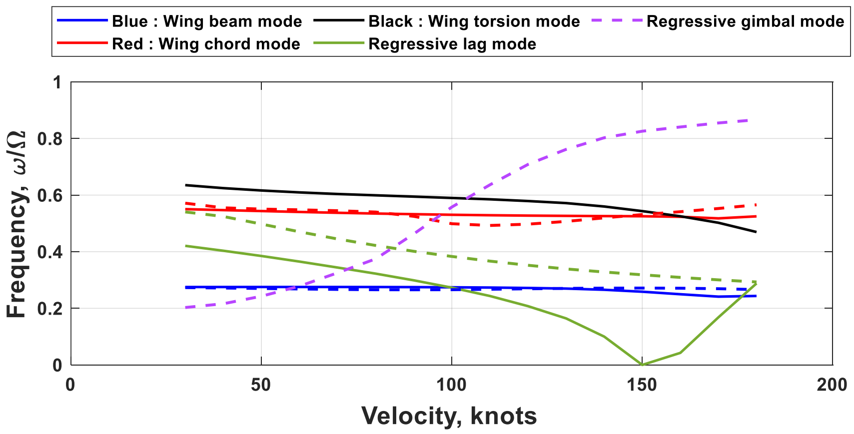

(a) Frequency

DOI: 10.13009/EUCASS2023-345

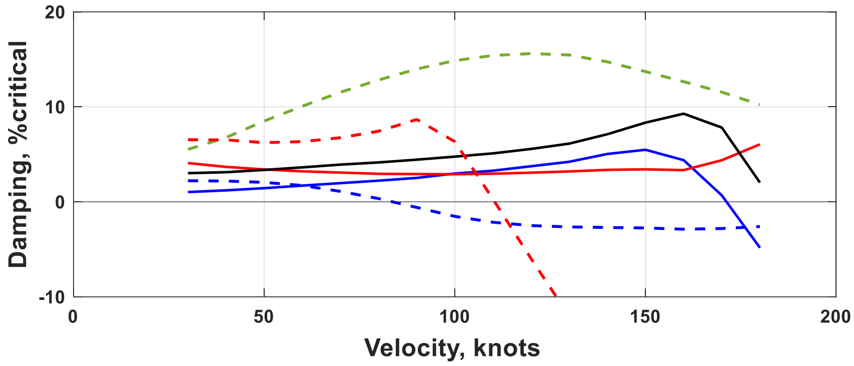

(b) Damping

Figure 6: Whirl flutter analysis results for gimballed and TRAST stiff in-plane hingeless and gimballed tiltrotors (solid line : hingeless rotor, dashed line : gimballed rotor)

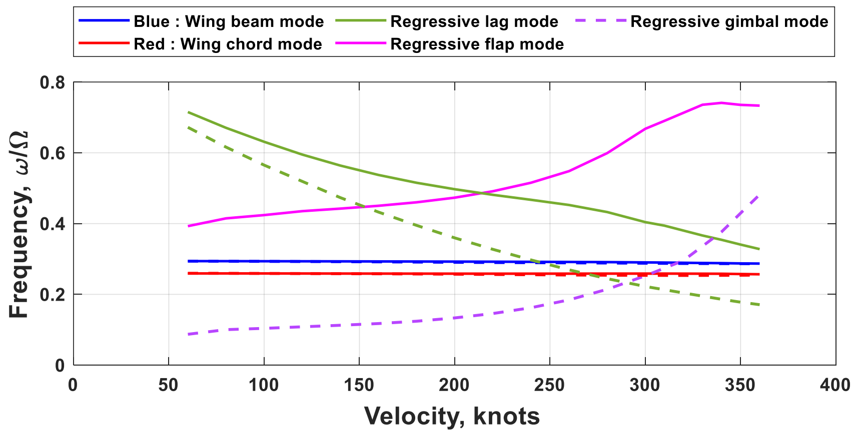

(a) Frequency

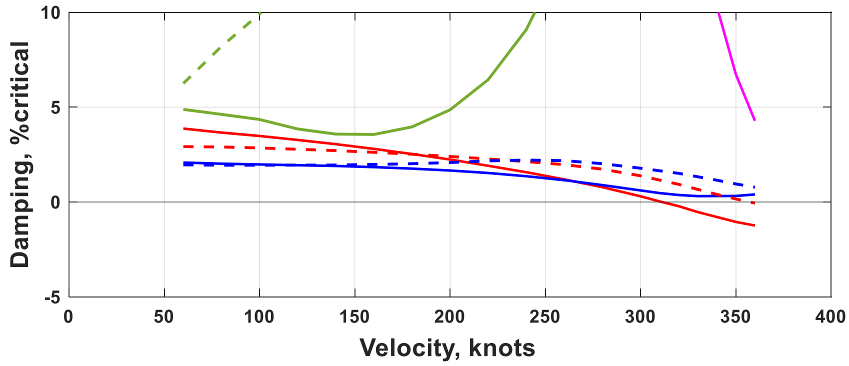

(b) Damping

Figure 7: Whirl flutter analysis results for gimballed and TRS stiff in-plane hingeless and gimballed tiltrotors (solid line : hingeless rotor, dashed line : gimballed rotor)

DOI: 10.13009/EUCASS2023-345

4. Conclusion

This study investigated the gimbal and hingeless proprotor whirl flutter characteristics of a tiltrotor in airplane mode using the comprehensive rotorcraft analysis code, CAMRAD II. The TRAST hingeless rotor and generic wing/pylon model developed by the U.S. Army and NASA were used as the baseline hingeless tiltrotor model. The models included soft in-plane and stiff in-plane rotors. In addition, the TRS stiff in-plane gimballed rotor and its wing/pylon model developed by KARI were considered as another baseline tiltrotor model. The baseline hingeless and gimballed hub models were newly modified into gimbal and hingeless hubs, respectively. The present whirl flutter analysis technique using CAMRAD II was validated by comparison with previous analysis results for the TRAST soft in-plane hingeless rotor with the generic wing/pylon model using RCAS and UMARC II. The overall trends in the frequency and damping values for the wing and rotor modes were predicted similarly in all analyses. For the TRAST soft in-plane rotor, the instability of the wing mode occurred in the wing chord mode for both hub models. The whirl flutter phenomenon for the hingeless hub was generated via the interaction of the wing chord mode and rotor collective lag mode at 85 knots. However, only for the gimballed hub model, the damping in the rotor regressive lag mode became unstable at 55 knots owing to the intersection between the rotor regressive lag and regressive gimbal modes. In the two stiff in-plane rotor models, the whirl flutter speed was 85 knots higher for the TRAST hingeless model than for the TRAST gimballed rotor and 50 knots higher for the TRS gimballed model than for the TRS hingeless rotor. For the hingeless hub models, the rotor regressive lag mode affected the wing mode that caused whirl flutter, which was commonly observed for both the TRAST and TRS tiltrotors. In contrast, for the gimballed rotor, the wing mode instability was caused by the frequency cross-over between the rotor regressive gimbal mode and wing mode. In summary, the whirl flutter behavior differed for the hub types. For a hingeless hub, wing mode instability was generated by the frequency intersection between the rotor regressive lag or collective lag mode and the wing modes. By contrast, the rotor regressive gimbal mode primarily had an influence on the wing and rotor modes, causing instability in the wing or rotor. This indicated that the wing-rotor interaction behavior that leads to whirl flutter differs depending on the type of rotor hub. In this study, it was shown that the frequency in the rotor regressive lag or collective lag mode was an important system design parameter for the tiltrotor using a hingeless hub; however, for gimballed hubs, the frequency in the rotor regressive gimbal mode was important. Therefore, the primary rotor mode depending on the hub type must be properly identified, and the tiltrotor should be designed to properly arrange the frequency in the primary rotor and wing modes to increase the whirl flutter speed.

Acknowledgments

This study was supported by Basic Science Research Program through the National Research Foundation of Korea (NRF) funded by the Ministry of Education (2020R1I1A3071793). This research was supported by Basic Science Research Program funded by Ministry of Science and ICT (2021R1A5A1031868).

References

[1] Weisgerber, M. 2022. Army chooses bell v-280 to replace its black hawk helicopters. *Defense One*, available at: https://www.defenseone.com/business/2022/12/army-chooses-bell-v-280-replace-its-black-hawkhelicopters/380487/ (accessed 23 January 2023)

[2] Johnson, W., Lau, B. H., and Bowles, J. V. 1986. Calculated performance, stability and maneuverability of high-speed tilting-prop-rotor aircraft. *NASA-TM-88349*.

[3] Taylor, E. S., and Browne, K. A. 1938. Vibration isolation of aircraft power plants. *J. eronautical Sciences*. 6:43–49.

[4] Kreshock, A. R., Acree, C. W., Kang, H., and Yeo, H. 2019. Development of a new aeroelastic tiltrotor wind tunnel testbed. In: *AIAA Scitech 2019 Forum*.

[5] Johnson, W. 1974. Dynamics of tilting proprotor aircraft in cruise flight. *NASA-TN-D-7677*.

[6] Nixon, M. W., Langston, C. W., Singleton, J. D., Piatak, D. J., Kvaternik, R. G., Corso, L. M., and Brown, R. K. 2003. Aeroelastic stability of a four-bladed semi-articulated soft-inplane tiltrotor model. In : *International Forum on Aeroelasticity and Structural Dynamics*.

[7] Yeo, H., and Kreshock, A. R. 2020. Whirl flutter investigation of hingeless proprotors. *J. Aircraft*. 57:586-596.

[8] Hohenemser, K. H. 1974. Hingeless rotorcraft flight dynamics. *Agardograph*. 197.

[9] Maisel, M. D., Giulianetti, D. J., and Dugan, D. C. 2000. The history of the XV-15 tiltrotor research aircraft: From concept to flight. *NASA-SP-2000-4517*.

[10] Hall, W. E. 1966. Prop-rotor stability at high advance ratios. *J. American Helicopter Society*. 11:11–26.

DOI: 10.13009/EUCASS2023-345

[11] Acree Jr, C. W., Peyran, R. J., and Johnson, W. 2004. Rotor design options for improving XV-15 whirl-flutter stability margins. *NASA/TP-2004-212262*.
[12] Piatak, D. J., Kvaternik, R. G., Nixon, M. W., Langston, C. W., Singleton, J. D., Bennett, R. L., and Brown, R. K. 2002. A parametric investigation of whirl-flutter stability on the WRATS tiltrotor model. *J. American Helicopter Societ*. 47:134–144.
[13] Acree Jr, C. W. 2002. Rotor design options for improving V-22 whirl-mode stability. In: *American Helicopter Society 58th Annual Forum*, 2095-2110.
[14] Yeo, H., Kang, H., and Kreshock, A. R. 2021. Modeling and analysis of proprotor whirl flutter. In: *Vertical Flight Society's 77Th Annual Forum & Technology Display*.
[15] Kreshock, A. R., Thornburgh, R., and Wilbur, M. 2022. Overview of the tiltrotor aeroelastic stability testbed. In: *AIAA SCITECH 2022 Forum*.
[16] Gul, S. 2022. A modern aeromechanical analysis of hingeless hub tiltrotors with model-and full-scale wind tunnel validation. Doctor of Philosophy. *University of Maryland*.
[17] Kim, D. H., Lee, J. Y., Kim Y. S., Lee M. K., and Kim, S. H. 2006. Rotor aeroelastic and whirl flutter stability analysis for smart-UAV. *J. Korean Society Aeronautical and Space Sciences*. 34:75-82.
[18] Lee, M. K., and Shen, J. 2008. Rotor stability and whirl flutter analysis of Smart UAV. *J. Aerospace Engineering and Technology*. 7:205-212.